THYROID
Volume 24, Number 7, 2014

DOI: 10.1089/thy.2014.0014

Bioluminescent Human Thyrospheres Allow Noninvasive Detection of Anaplastic Thyroid Cancer Growth and Metastases *In Vivo*

Ashley N. Reeb, Wen Li, and Reigh-Yi Lin

Background: We have previously demonstrated that thyrospheres derived from human anaplastic thyroid cancer (ATC) cell lines can reconstitute and sustain tumor growth *in vivo*. The aim of this study was to use luciferase-expressing thyrospheres to establish a clinically relevant mouse model of ATC that allows noninvasive and sensitive monitoring of tumor progression.
Methods: Two human ATC cell lines stably transfected with a firefly *luciferase* gene were used to generate thyrospheres under stem cell culture conditions. Cells were orthotopically implanted into the thyroids of immunodeficient *NOD/SCIDIl2rg-/-* mice to initiate tumors. Tumor progression and metastasis were evaluated by bioluminescent imaging weekly as well as histologic analysis postmortem.
Results: We show that only 100 thyrosphere cells are needed for tumor development, and that tumors can be monitored with bioluminescent imaging as early as 7–14 days after implantation. Subsequent histologic evaluation of tissue sections confirmed characteristics of high-grade malignant neoplasms.
Conclusions: This approach offers rapid and highly sensitive noninvasive detection options for the preclinical assessment of novel ATC therapeutics *in vivo*.

Introduction

Anaplastic thyroid cancer (ATC) is a rare but highly lethal form of thyroid cancer with a mean survival time of less than 6 months from the time of diagnosis. The major challenges of ATC are represented by a lack of diagnostic tools for early detection and a poor response to all current treatment modalities (1,2). ATC is an undifferentiated thyroid cancer that has traditionally been thought to dedifferentiate from well-differentiated thyroid cancers, including papillary and follicular thyroid cancer (3,4). However, emerging evidence indicates that ATC contains a small subset of cancer stem-like cells that have the ability to grow as nonadherent thyrospheres and sustain self-renewal in culture (3,5–11). We recently evaluated four bona fide human ATC cell lines (THJ-11T, THJ-16T, THJ-21T, and THJ-29T) and showed that approximately 3–9% percent of cells from these cell lines formed thyrospheres when seeded in stem-cell–culture conditions on ultra-low attachment plates. These thyrosphere cells are tumorigenic and, in an orthotopic mouse model of ATC, they metastasize more aggressively than cells derived from the parental monolayer (5). To further our analysis, we describe here the use of bioluminescent human thyrospheres to establish a clinically relevant mouse model of ATC that allows noninvasive and sensitive monitoring of tumor progression and drug response over time.

In recent years, xenografting of firefly luciferase-labeled cancer cells followed by bioluminescent imaging has offered unique optical imaging opportunities to monitor tumor metastases in living animals. Bioluminescence provides a noninvasive and sensitive way to follow cell trafficking and tumor growth *in vivo* and it has enormous potential when used as a tool to accurately evaluate the outcome of a given pharmacologic intervention. Here, we engineered a *luciferase* gene into THJ-11T and THJ-16T cell lines to generate stable clones. These clones were used to generate luciferase-expressing thyrosphere cells, which were subsequently orthotopically implanted into the thyroid of *NOD/SCIDIl2rg-/-* mice to initiate tumors. Tumor progression and metastasis were evaluated by live bioluminescent imaging weekly as well as histologic analysis postmortem.

Materials and Methods

Cell culture, transfection, and generation of thyrospheres

Human ATC cell lines THJ-11T and THJ-16T (12) were provided by Dr. John Copland of the Mayo Clinic. Cells were cultured in RPMI-1640 medium (Cellgro, Manassas, VA) supplemented with 10% fetal bovine serum. Cells were transfected with vector expressing the firefly *luciferase* gene (pSIN-luc; a gift of Dr. Yasuhiro Ikeda of the Mayo Clinic) to

Department of Otolaryngology–Head and Neck Surgery, Saint Louis University School of Medicine, Saint Louis, Missouri.

FIG. 1. *In vitro* bioluminescence of THJ-11T and THJ-16T cells. Stable clones of THJ-11T and THJ-16T cells expressing luciferase were serially diluted in duplicate wells from 50,000 to 1000 cells per well. Luciferin substrate was added to each well 10 minutes before imaging and the plate was imaged to obtain photons/s per cell. Wells with media but not cells, or cells alone without luciferin, were included as controls **(A)**. Note the level of luciferase expression was proportional to the number of cells seeded **(B)**.

FIG. 2. *In vivo* bioluminescence of THJ-11T and THJ-16T cells in immunodeficient mice. **(A)** THJ-11T– and THJ-16T-luciferase–expressing cells (500,000 cells per mouse) were injected into the right thyroid of *NOD/SCIDIl2rg*$^{-/-}$ mice, and tumor growth and metastasis were monitored over time *in vivo*. Tumor take rate was 100% (4/4 mice per cell line). **(B)** Bioluminescent images were taken using an IVIS Spectrum. All mice were reimaged using the same setting of IVIS Spectrum and bioluminescent signals were quantified as total flux photons/s (p/s) using Living Image software and plotted against the days since implantation. **(C)** Histologic analysis of the tumor tissue confirmed invasion to the trachea, smooth muscles, and the esophagus. Tumors displayed with a mixed morphology of spindle cells and pleomorphic giant cells. Scale bar, 100 μm.

generate stable clones. Isolated clones were screened for luciferase activities in complete media supplemented with 150 μg/mL luciferin (Gold Biotechnology, St. Louis, MO) using an IVIS Spectrum (Caliper Life Sciences, Hopkinton, MA). A detailed description of the construction and transfection protocol has been previously published (13). To obtain thyrospheres, single cells were plated at 5000 cells per well on ultra-low attachment six-well plates (Fisher Scientific International, Hampton, NH) and thyrospheres were harvested after 7 days as described previously (5).

Animals and ethics statement

Eight-week-old female *NOD/SCIDIl2rg-/-* mice were obtained from Charles River (Boston, MA) and maintained under pathogen-free conditions at Saint Louis University Animal Facility. This study was carried out in strict accordance with the recommendations in the Guide for the Care and Use of Laboratory Animals of the National Institutes of Health. The protocol was approved by the Institutional Animal Care and Use Committee (IACUC) of Saint Louis University (Protocol Number: 2207). All procedures were in accordance with institutional animal welfare guidelines, and all efforts were made to minimize suffering.

Mice and tumor cell implantation

For orthotopic transplantation, thyrospheres were trypsinized into single cells and resuspended in 10 μL of Matrigel/RPMI (Matrigel; Corning Life Sciences, Tewksbury, MA) at a 1:1 dilution and implanted into the right thyroid gland of *NOD/SCIDIl2rg-/-* mice (14). Mice were sacrificed when the animals lost approximately 20% of their body weight and displayed signs of severe cachexia. Tumors and adjacent tissues were collected and analyzed for metastasis by routine histology.

Bioluminescent imaging

Bioluminescent imaging was performed with an IVIS Spectrum using a protocol similar to those described previously (15). The light emitted from the bioluminescent tumors was detected, digitized and displayed and regions of interest from displayed images were quantified as total photon counts (photons/s) using Living Image software (Caliper Life Sciences).

Statistical analysis

Statistical analysis was performed using Prism 5.0 software (GraphPad Software, La Jolla, CA). Numerical data are expressed as mean ± standard error of the mean (SEM). Statistical differences are considered significant at $p < 0.05$.

Results

Stable luciferase expression by THJ-11T and THJ-16T cell lines

THJ-11T and THJ-6T cells were transfected with a pSIN-luc vector encoding a firefly *luciferase* gene (13) and several stable clones from each cell line were selected for further analysis. Three bioluminescent clones from each cell line were chosen for further analyses. The luciferase activities of serial dilutions of cell cultures of each clone were analyzed and compared *in vitro*. The level of luciferase expression was proportional to the number of cells seeded (Fig. 1).

Tumor development and metastasis from luciferase-expressing THJ-11T and THJ-16T cells

We next attempted to detect tumor growth and metastasis *in vivo* of labeled THJ-11T and THJ-16T cells after implantation into groups of *NOD/SCIDIl2rg-/-* mice (5×10^5 cells per mouse, $n = 4$ per cell line). This cell number has been

FIG. 3. Tumors detected *in vivo* following intrathyroidal injection of THJ-11T and THJ-16T thyrospheres in mice. **(A)** THJ-11T– and THJ-16T–luciferase expressing thyrosphere cells were injected into the right thyroid of *NOD/SCIDIl2rg-/-* mice, and tumor growth and metastasis were monitored over time *in vivo*. Tumor take rate was 100% (4/4 mice per group). Bioluminescent images were taken weekly. **(B)** The noninvasive light imaging detected the tumors arising from as few as 100-cell implantation at day 7–14, and the total flux from the implantation sites was directly proportional to the number of cells implanted. **(C)** Histologic analysis of the tumor tissue confirmed invasion to adjacent tissues and tumors displayed a high-grade malignant neoplasm characterized by necrosis and marked pleomorphism (arrows). Scale bar, 100 μm.

Figure 1

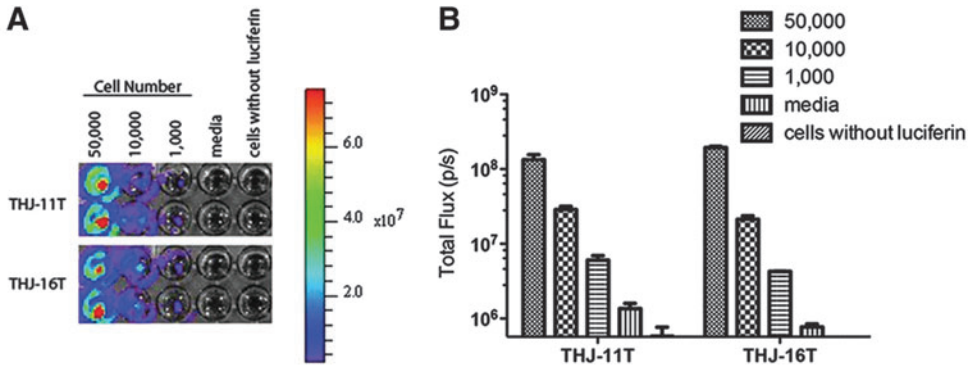

Figure 2

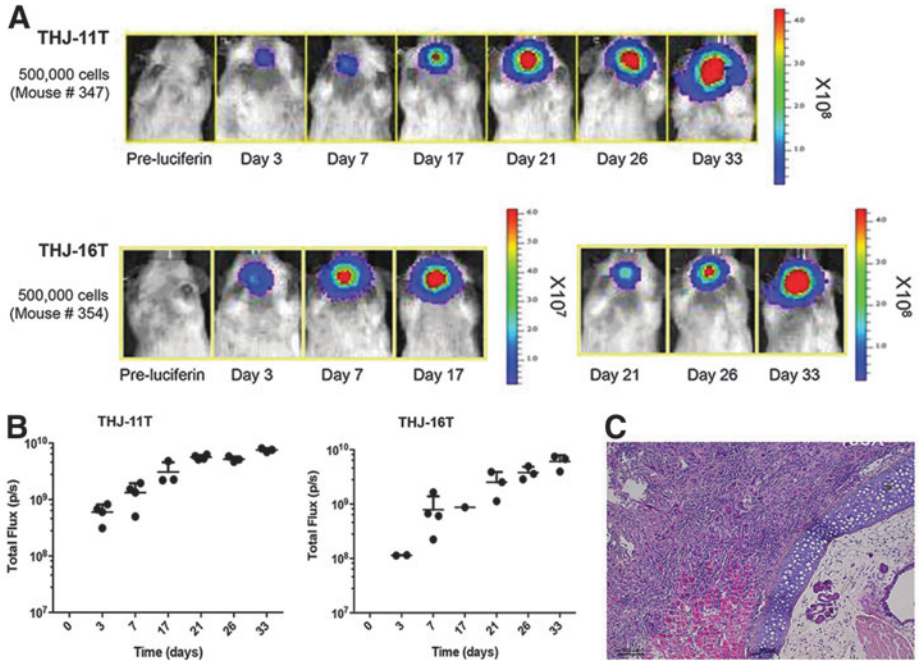

Figure 3

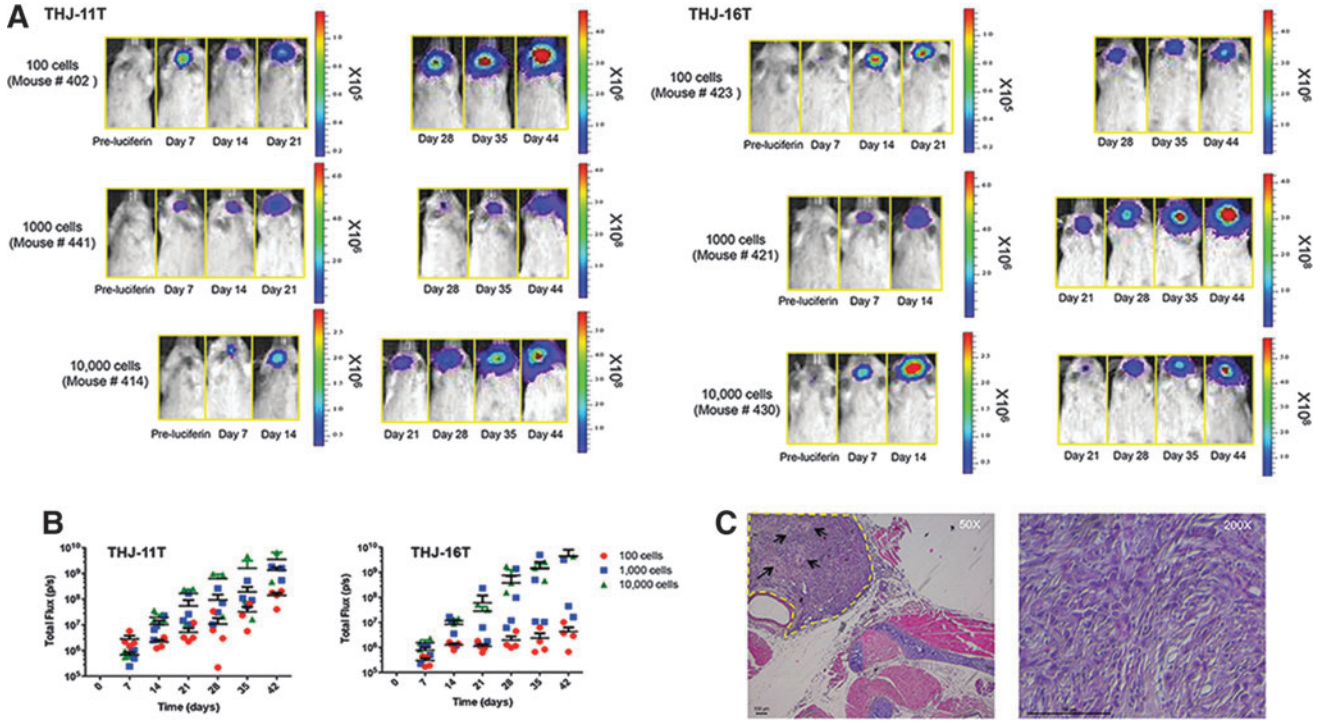

shown in our previous studies to be sufficient to cause tumor development in these mice (5). Using an IVIS Spectrum imaging system, we were able to detect bioluminescent signals at the implantation sites in all the mice (Fig. 2). The tumors grew rapidly and developed metastatic lesions that could be detected with bioluminescent imaging as early as 3 days after implantation. They remained detectable until around 33 days, when most of the mice displaying signs of severe cachexia and were sacrificed after losing more than 20% of their body weight. Histologic analysis of the tumors identified many clinical features of ATC—a high-grade malignant neoplasm characterized by a high mitotic index, nuclear atypia, cellular pleomorphism, and necrosis. Mice also developed extrathyroidal invasions to the trachea, smooth muscles, and the esophagus (Fig. 2).

Tumors detected in vivo *after intrathyroidal injection of THJ-11T and THJ-16T thyrospheres in mice*

After confirming the ability to noninvasively detect bioluminescent THJ-11T and THJ-16T cells *in vivo*, we attempted to use bioluminescent imaging to detect and track a small number of thyrosphere cells to investigate the hypothesis that ATC contains cancer stem-like cells. We previously demonstrated that 10,000 thyrosphere cells (a cell number 50-fold less than that required when using parental monolayer THJ-11T cells) injected into the thyroid can cause tumor development in mice (5). Here we explored the effect of implanting varying numbers of luciferase-expressing THJ-11T– and THJ-16T–derived thyrosphere cells (100, 1000, and 10,000 cells per mouse, $n=4$ per cell line) into the thyroids of *NOD/SCIDIl2rg-/-* mice. Seven days after implantation, all mice developed tumors—a 100% success rate for tumor initiation regardless of the number of cells implanted (Fig. 3). More importantly, we were able to detect tumors arising from as few as 100 cells after only 7 to 14 days. The total flux from the implantation sites was directly proportional to the number of cells implanted (Fig. 3). Histologic analysis of the orthotopic tumors arising from thyrospheres revealed tumors around the trachea and tracheal invasion into smooth muscle and esophagus, and hematoxylin and eosin staining confirmed these tumors are high-grade malignant neoplasms that share characteristics of ATC (Fig. 3). Together, these data clearly show that tumor growth and metastasis in an animal can be monitored using noninvasive bioluminescent imaging. Furthermore, it validates the cancer stem-like cell model of ATC, because even as few as 100 thyrosphere cells are sufficient to develop tumors in mice.

Discussion

Several mouse tumor models of ATC have been established, including subcutaneous and orthotopic xenografts of tumor cells implanted into immunodeficient mice. Subcutaneous xenograft models have been valuable for preclinical screening. However, this method is suitable only for palpable tumors growing under the skin of the animals and does not well reflect the metastasis seen in human disease. Orthotopic tumor xenograft models provide a more biologically relevant context in which to study the disease by implanting tumor cells directly into their equivalent anatomical origin in a host animal. (14,16). However, traditional orthotopic models are impractical for evaluation of drug efficacy since they require large numbers of animals to be sacrificed at each time point. In addition, accurate evaluation and quantitation of tumor burden can be difficult. In contrast, noninvasive whole-body bioluminescent imaging allows us to obtain information in real time without sacrificing the animals and response to treatment can be easily followed longitudinally in a single animal throughout the study. The ability to obtain sequential images of a single animal could yield valuable insight to tumor progression and provide a significant advantage for evaluating therapeutic efficacy in preclinical disease models.

In the present study, we report the first development of mouse models of ATC with bioluminescent human thyrospheres. As few as 100 cells from the ATC thyrospheres were able to form a tumor when orthotopically injected into *NOD/SCIDIl2rg-/-* mice, whereas at least 5×10^5 parental cells were needed to generate a tumor in the same model. This was 5000 times higher than that of sphere-forming cells. This model allows the comparison of the effectiveness of a given pharmacologic intervention on early stages of ATC and metastases. It can also serve as a valuable tool for the investigation of biologic processes and the development of novel therapies of ATC in preclinical models.

Acknowledgments

We thank Dr. John A. Copland for ATC cell lines, Dr. Yasuhiro Ikeda for pSIN-luc vector, and Dr. Ling-Jun Zhao for technical assistance with luciferase transfection. We also thank Dr. Karoly Toth and the Saint Louis University Animal Imaging Core Facility for assistance with IVIS imaging. This work was supported by the President's Research Fund of Saint Louis University (to R.Y.L.).

Author Disclosure Statement

No competing financial interests exist.

References

1. Smallridge RC, Ain KB, Asa SL, Bible KC, Brierley JD, Burman KD, Kebebew E, Lee NY, Nikiforov YE, Rosenthal MS, Shah MH, Shaha AR, Tuttle RM; American Thyroid Association Anaplastic Thyroid Cancer Guidelines Taskforce 2012 American Thyroid Association guidelines for management of patients with anaplastic thyroid cancer. Thyroid **22:**1104–1139.
2. Smallridge RC, Copland JA 2010 Anaplastic thyroid carcinoma: pathogenesis and emerging therapies. Clin Oncol (R Coll Radiol) **22:**486–497.
3. Lin RY 2011 Thyroid cancer stem cells. Nat Rev Endocrinol **7:**609–616.
4. Patel KN, Shaha AR 2006. Poorly differentiated and anaplastic thyroid cancer. Cancer Control **13:**119–128.
5. Li W, Reeb AN, Sewell WA, Elhomsy G, Lin RY 2013 Phenotypic characterization of metastatic anaplastic thyroid cancer stem cells. PLoS One **8:**e65095.
6. Todaro M, Iovino F, Eterno V, Cammareri P, Gambara G, Espina V, Gulotta G, Dieli F, Giordano S, De Maria R, Stassi G 2010 Tumorigenic and metastatic activity of human thyroid cancer stem cells. Cancer Res **70:**8874–8885.
7. Malaguarnera R, Morcavallo A, Giuliano S, Belfiore A 2012 Thyroid cancer development and progression: emerging role of cancer stem cells. Minerva Endocrinol **37:**103–115.

8. Thomas D, Friedman S, Lin RY 2008 Thyroid stem cells: lessons from normal development and thyroid cancer. Endocr Relat Cancer **15:**51–58.
9. Klonisch T, Hoang-Vu C, Hombach-Klonisch S 2009 Thyroid stem cells and cancer. Thyroid **19:**1303–1315.
10. Zheng X, Cui D, Xu S, Brabant G, Derwahl M 2010 Doxorubicin fails to eradicate cancer stem cells derived from anaplastic thyroid carcinoma cells: characterization of resistant cells. Int J Oncol **37:**307–315.
11. Hardin H, Montemayor-Garcia C, Lloyd RV 2013 Thyroid cancer stem-like cells and epithelial-mesenchymal transition in thyroid cancers. Hum Pathol **44:**1707–1713.
12. Marlow LA, D'Innocenzi J, Zhang Y, Rohl SD, Cooper SJ, Sebo T, Grant C., McIver B, Kasperbauer JL, Wadsworth JT, Casler JD, Kennedy PW, Highsmith WE, Clark O, Milosevic D, Netzel B, Cradic K, Arora S, Beaudry C, Grebe SK, Silverberg ML, Azorsa DO, Smallridge RC, Copland JA 2010 Detailed molecular fingerprinting of four new anaplastic thyroid carcinoma cell lines and their use for verification of RhoB as a molecular therapeutic target. J Clin Endocrinol Metab **95:**5338–5347.
13. Hasegawa K, Nakamura T, Harvey M, Ikeda Y, Oberg A, Figini M, Canevari S, Hartmann LC, Peng KW 2006 The use of a tropism-modified measles virus in folate receptor-targeted virotherapy of ovarian cancer. Clin Cancer Res **12:**6170–6178.
14. Sewell W, Reeb A, Lin RY 2013 An orthotopic mouse model of anaplastic thyroid carcinoma. J Vis Exp Apr 17;(74).
15. Jenkins DE, Hornig YS, Oei Y, Dusich J, Purchio T 2005 Bioluminescent human breast cancer cell lines that permit rapid and sensitive in vivo detection of mammary tumors and multiple metastases in immune deficient mice. Breast Cancer Res **7:**R444–454.
16. Nucera C, Nehs MA, Mekel M, Zhang X, Hodin R, Lawler J, Nose V, Parangi S 2009 A novel orthotopic mouse model of human anaplastic thyroid carcinoma. Thyroid **19:**1077–1084.

Address correspondence to:
Reigh-Yi Lin, PhD
Department of Otolaryngology–Head and Neck Surgery
Saint Louis University School of Medicine
1100 South Grand Boulevard
Saint Louis, MO 63104

E-mail: rlin7@slu.edu